Thermochimica Acta, 185 (1991) 155–169
Elsevier Science Publishers B.V., Amsterdam

The copper–lead phase diagram

Osmo Teppo *, Jaana Niemelä ** and Pekka Taskinen *

Helsinki University of Technology, Faculty of Process Engineering and Materials Science, Laboratory of Materials Processing and Powder Metallurgy, SF-02150 Espoo (Finland)

(Received 17 December 1990)

Abstract

The thermodynamic properties of solid and liquid copper–lead alloys at 25–1200 °C have been critically analysed from the available literature sources. The excess Gibbs energies for the alloy phases have been optimised using least-squares methods by the Lukas program. The calculated phase diagram and a complete set of the excess Gibbs energy expressions are presented in addition to the limiting activity coefficients of the components at infinite dilution in the molten alloy.

INTRODUCTION

The phase diagram data of the copper–lead system were reviewed by Hansen and Anderko in 1958 [1] and further supplements have been published [2,3]. An assessment of the thermodynamic properties of molten copper–lead alloys was published by Hultgren et al. [4]. In addition, an interim assessment is available [5] and, more recently, comprehensive thermodynamic analyses have been carried out independently by Chakrabarti and Laughlin [6] and Niemelä et al. [7].

LITERATURE DATA

The phase diagram

The melting point of pure copper is 1084.87 °C (1358.02 K) and that of pure lead is 327.50 °C (600.65 K) [8]. They both crystallise in an fcc lattice of the same type, characterised by the Pearson symbol cF4 [9].

Copper and lead form a monotectic equilibrium at about 952 °C [1] above which a shallow liquid state immiscibility region is developed, of maximum range from about 21 at.% Pb to about 63 at.% Pb in the alloy [6]. According

* Outokumpu Group, Science and Technology, P.O. Box 27, SF-02201 Espoo, Finland.
** Kemira Oy, Oulu Research Centre, P.O. Box 171, SF-90101, Oulu, Finland.

0040-6031/91/$03.50

to Hansen and Anderko [1], the critical point of the miscibility gap lies slightly below 1000 °C at a composition of 40 at.% Pb. The relatively high critical temperature (> 1500 °C) obtained by Bornemann and Wagenmann [10] from their electrical resistivity measurements is most certainly incorrect. Chaib and Gasser [11] reported recently on the electrical resistivities of molten Cu–Pb alloys, indicating that the critical temperature is close to 1000 °C at about $x_{Pb} = 0.4$.

Since the reviews by Hansen and Anderko [1], Elliot [2] and Shunk [3], a few experimental investigations on the location of the phase boundaries above the monotectic temperature have been published.

The system forms a eutectic point close to pure lead and its melting temperature, the composition of the eutectic point being 99.8 at.% Pb [1]. Since the previous assessments, additional experimental points have been made available by Taskinen and Holopainen [12]. They used e.m.f. techniques in oxygen-bearing alloys with a low oxygen concentration. Marcotte and Schroder [13] measured accurately a few phase diagram points in lead-rich alloys using DSC. In addition, some older studies [14–17] were included in the experimental file.

The observations on the solid solubility of lead in copper and copper in lead are very limited [2,3,5,6] and insufficient for an accurate estimation of the phase relations in the terminal regions. The only experimental point on the copper terminal solution has been reported by Raub and Engel [18] at 600 °C with a solid solubility of 0.09 at.% $[Pb]_{Cu}$. The large solid solubility reported by Kim and Abdeev [19] on the basis of their vapour pressure measurements has not been confirmed by other authors. For the lead terminal solution, a solid solubility of less than 0.02 at.% $[Cu]_{Pb}$ has been reported [20].

Thermodynamic properties of the alloys

All the literature data available on the solution thermodynamics of copper–lead alloys have been referred to by Chakrabarti and Laughlin [6] and by Niemelä et al. [7]. A few experimental points obtained by using a transportation technique at 1200 °C have been reported by Roine and Jalkanen [21]. In addition, Esdaile and McAdam [22] have recalculated the chemical potential of lead in the liquid alloy using the vapour pressure data of Abdeev and Miller [23].

THE LEAST-SQUARES OPTIMISATION

The solution models

Pure mathematical solution models using Redlich–Kister polynomials [24] were used to express the excess Gibbs energies of the alloy phases. In

the optimisation, the molten alloy and the fcc copper terminal solution were treated as alloy phases and the minor solid solubility of copper in lead was neglected.

The analytical form of the integral Gibbs energies for binary substitutional alloy phases can be written as

$$G = x_1 G_1^{\ominus} + x_2 G_2^{\ominus} + RT\left[x_1 \ln (x_1) + x_2 \ln (x_2)\right] + {}^{Ex}G \tag{1}$$

with

$${}^{Ex}G = x_1 x_2 \sum A_i z^i \tag{2}$$

where $G_i^{\ominus}$ is the lattice stability of component i, A_i are adjustable parameters and $z = x_1 - x_2 = x_{Cu} - x_{Pb}$.

The temperature dependences of the model parameters A_i were expressed by assuming negligible Δc_p for the formation of the alloy phases, i.e. by adopting for the parameters

$$A_i = A_{i0} + A_{i1} T \tag{3}$$

where A_{i0} and A_{i1} are coefficients to be calculated from the experimental data.

Optimisation of the model parameters

The Lukas least-squares optimisation program [25], the module BINGSS updated 27 July 1989, was used for the assessment and fitting of the experimental information. The phase diagrams were calculated using the program BINFKT, the version updated 16 August 1989, kindly provided by Dr H.-L. Lukas from the Max-Planck-Institut für Metallforschung in Stuttgart.

The SGTE lattice stabilities of pure copper and lead according to Dinsdale [26] were used. The temperature dependences of their Gibbs energies were given by the expression

$$G^{\ominus} = A + BT + CT \ln T + DT^2 + E/T + FT^3 + IT^4 + JT^7 + KT^{-9} \tag{4}$$

where A–K are coefficients specific to each element and lattice form.

The coefficients in eqn. (4) for fcc and liquid copper and lead used in the present calculations can be found in Table 1.

The experimental information and the accuracies used in the final optimisation are listed in Table 2. In most cases, the errors adopted were based on the experimental values published but, occasionally, larger errors justified by the optimisation procedure were used.

Owing to the very limited solubility range, the fcc copper terminal solution was assumed to obey the pure regular solution behaviour. For the

TABLE 1

Coefficients of the lattice stability functions and their temperature intervals for pure copper and lead used in the calculations [26]; reference state SER (J mol^{-1})

A	*B*	*C*	*D*
Cu(liquid)			
298.15–1358.02 K			
5.19438200E+03	1.20975160E+02	−2.41123920E+01	−2.65684000E−03
1358.02K			
−4.69300000E+01	1.73883734E+02	−3.13800000E+01	0.00000000E+00
Cu(fcc)			
298.15–1358.02 K:			
−7.77045800E+03	1.30485403E+02	−2.41123920E+01	−2.65684000E−03
1358.02 K			
−1.35423300E+04	1.83804197E+02	−3.13800000E+01	0.00000000E+00
Pb(liquid)			
298.15–600.65 K			
−2.97792800E+03	9.39649310E+01	−2.45242231E+01	−3.65895000E−03
600.65–1200.00 K			
−5.67800300E+03	1.46191568E+02	−3.24913959E+01	1.54613000E−03
1200.00 K			
9.01070800E+03	4.50874580E+01	−1.89640637E+01	−2.88294300E−03
Pb(fcc)			
298.15–600.65 K			
−7.65008500E+03	1.01715188E+02	−2.45242231E+01	−3.65895000E−03
600.65–1200.00 K			
−1.05311150E+04	1.54258155E+02	−3.24913959E+01	1.54613000E−03
1200.00 K			
4.15759600E+03	5.31540450E+01	−1.89640637E+01	−2.88294300E−03

molten alloy, a fourth-degree Redlich–Kister polynomial was found to be necessary to reproduce the experimental liquid state miscibility gap.

RESULTS AND DISCUSSION

The optimised set of Redlich–Kister coefficients, according to eqns. (1) and (3), for the integral excess Gibbs energies of the alloy phases are given in Table 3. Owing to insufficient experimental data on the fcc copper terminal solution, the regular solution parameter given must be taken as tentative only and as an attempt to express the thermodynamic solution properties in the analytical form needed for the phase diagram calculations.

The phase diagram

The calculated phase diagram is shown in Fig. 1 together with the experimental points. A detail in Fig. 2 shows the calculated phase relations

E	*F*	*I*	*J*	*K*
5.2478000E+04	1.2922300E−07	0.000000E+00	−5.839320E−21	0.000000E+00
0.0000000E+00	0.0000000E+00	0.000000E+00	0.000000E+00	0.000000E+00
5.2478000E+04	1.2922300E−07	0.000000E+00	0.000000E+00	0.000000E+00
0.0000000E+00	0.0000000E+00	0.000000E+00	0.000000E+00	3.646430E+29
0.0000000E+00	−2.4395000E−07	0.000000E+00	−6.014400E-19	0.000000E+00
0.0000000E+00	0.0000000E+00	0.000000E+00	0.000000E+00	0.000000E+00
−2.6967550E+0.6	9.8144000E−08	0.000000E+00	0.000000E+00	0.000000E+00
0.0000000E+00	−2.4395000E−07	0.000000E+00	0.000000E+00	0.000000E+00
0.0000000E+00	0.0000000E+00	0.000000E+00	0.000000E+00	8.056440E+25
−2.6967550E+06	9.8144000E−08	0.000000E+00	0.000000E+00	8.056440E+25

in the vicinity of the eutectic point at 326.5 °C (599.7 K). The assessed liquidus line is in good agreement with several independent series of measurements [12,13,15,17,28,33]. The points given by Vasil'ev [32] and Schürmann and Kaune [29] show systematic undercooling in lead-rich and copper-rich alloys, respectively, if compared with the assessed line. The largest scatter was found in the field of the liquid state miscibility gap, where an early study by Bornemann and Wagenmann [10] was excluded.

As a result of the optimisations the assessed critical point was found to be located at 1006.0 °C (1279.2 K) with a lead concentration of ${}^{cr}x_{Pb} = 0.31$. This is in fair agreement with the experimental points in Fig. 1 as well as with the earlier estimates [6,7,29], yielding slightly lower values for the critical temperature than were obtained in this work. As one can see, the assessed miscibility gap is non-symmetric which is also in accordance with the experimental points in refs. 29 and 14. Thus the value ${}^{cr}t = 1054\,°C$ obtained by Esdaile [39] as a result of modelling the liquidus curve only seems to be slightly too high. Accurate experimentation in the field of a

TABLE 2

Experimental data used in the optimisation: type of measurement and the estimated error

Phase diagram data	Thermodynamic measurements							Reference
	μ_{Pb}	μ_{Cu}	$d\mu$	$\Delta_{mix}H$	$d(\Delta H)$	dT (K)	dx (at.%)	
	+		10%			5	0.1	27
+						5	0.5	28
	+		200–250 J			5	1.5	28
				+	300 J	5	1.5	28
+						3	0.5	29
				+	300 J	5	1.0	29
		+	200–400 J			5	2.0	30
				+	20%	5	2.0	30
+						3	0.5	31
+						5	0.5	32
+						3	0.5	17
+						3	0.5	33
+						2	0.5	34
	+		20%			6	0.5	19
				+	500 J	6	1.5	35
	+		10%			6	3.0	36
+						5	0.5	37
+						3	1.0	12
+						6	1.0	15
+						6	1.0	16
+						3	0.5	13
+						8	1.0	14
	+		1500–2000 J			20	4.0	23
	+		10%			5	0.5	21
				+	500 J	6	1.5	38
+						5	0.01	18

TABLE 3

The assessed Redlich–Kister parameters for the excess Gibbs energies of the alloy phases (J mol^{-1})

i, j	A_{ij}	
	0	1
	Liquid	
0	27220.53	−4.43594
1	9405.87	−6.29287
2	−3946.32	5.07294
3	−23274.73	18.77941
4	−4611.25	
	Cu (fcc)	
0	49733.50	0

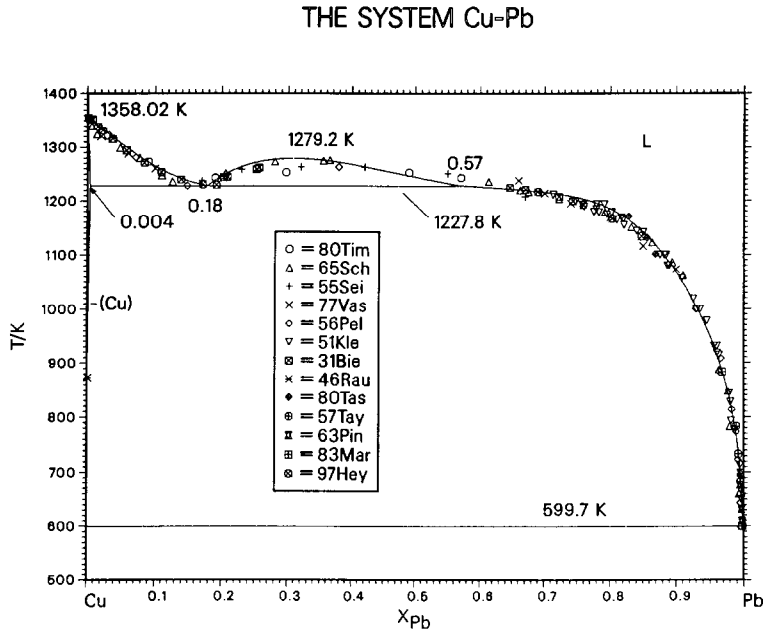

Fig. 1. Calculated phase diagram for the copper–lead system at 500–1400 K: 97Hey [14], 31Bie [34], 46Rau [18], 51Kle [33], 55Sei [31], 56Pel [17], 57Tay [15], 63Pin [16], 65Sch [29], 77 Vas [32], 80Tas [12], 80Tim [28], 83Mar [13], ——— this work (calculated).

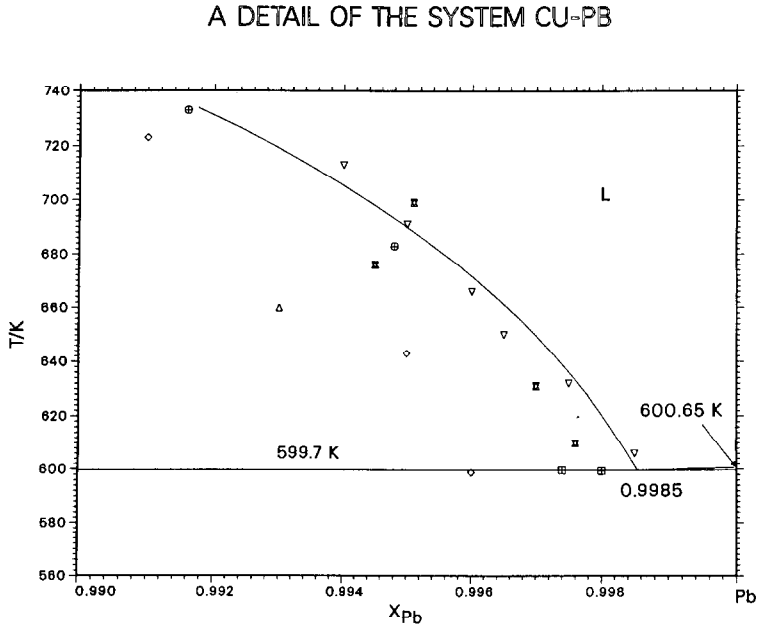

Fig. 2. Phase relations close to the eutectic point at 560–740 K in lead-rich alloys: symbols as in Fig. 1, ——— this work (calculated).

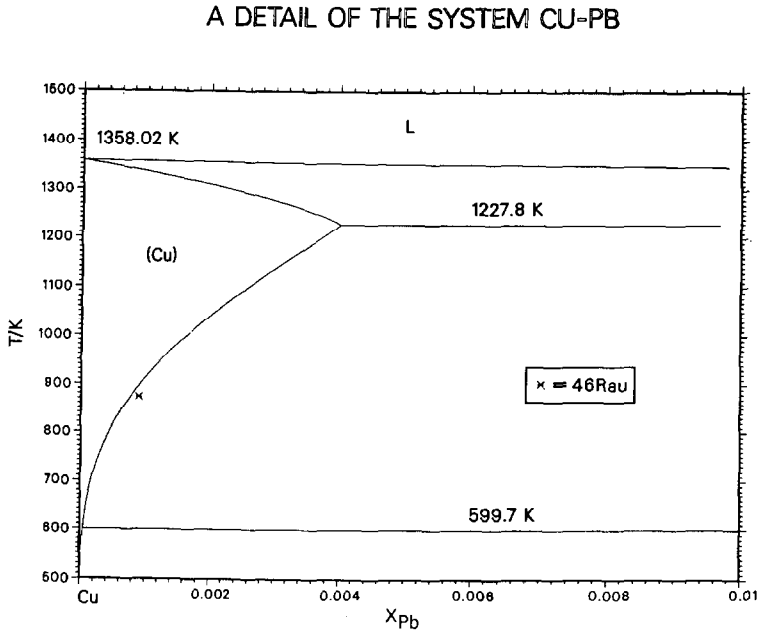

Fig. 3. The fcc terminal copper solid solution: 46Rau [18], ——— this work (calculated).

liquid state miscibility gap is, however, difficult and needs highly sensitive and reproducible techniques. Therefore, a critical examination of the experimental points and the methods used in this phase region is necessary.

The monotectic equilibrium was calculated as occurring at 954.6 °C (1227.8 K) with the monotectic points at ${}^{m'}x_{Pb} = 0.18$ and ${}^{m''}x_{Pb} = 0.570$. The value found is in good agreement with the experimental points of several authors [17,31,34]. Hansen and Anderko [1] and Chakrabarti and Laughlin [6] as well as Niemelä et al. [7] report highly concordant temperature values, but the lead-rich end of the miscibility gap in their estimates is above 60 at.% $[Pb]_{Cu}$. The copper-rich end of the miscibility gap obtained in the present work, see Fig. 1, is in good agreement with the assessed value given by Chakrabarti and Laughlin [6].

The eutectic point was calculated to be at 326.5 °C (599.7 K) with the eutectic composition being ${}^{e}x_{Pb} = 0.9985$. This value is in good agreement with the experimental observation obtained by Pelzel [40] who reported 599.2 K at $x_{Pb} = 0.9982$, and with the assessed values of Chakrabarti and Laughlin [6], 599 K at $x_{Pb} = 0.998$, and of Niemelä et al. [7], 598.67 K at ${}^{e}x_{Pb} = 0.9969$. The calculated liquidus line was at low temperatures in excellent agreement with the observations reported by Kleppa and Weil [33] and was only 10–20 K higher than those measured by Taylor [15], Pin and Wagner [16] and Pelzel [40].

Figure 3 compares the calculated fcc copper terminal solution with the available experimental information. As one can see, the experimental data on the solubility of lead in solid copper are scarce and further discussion on

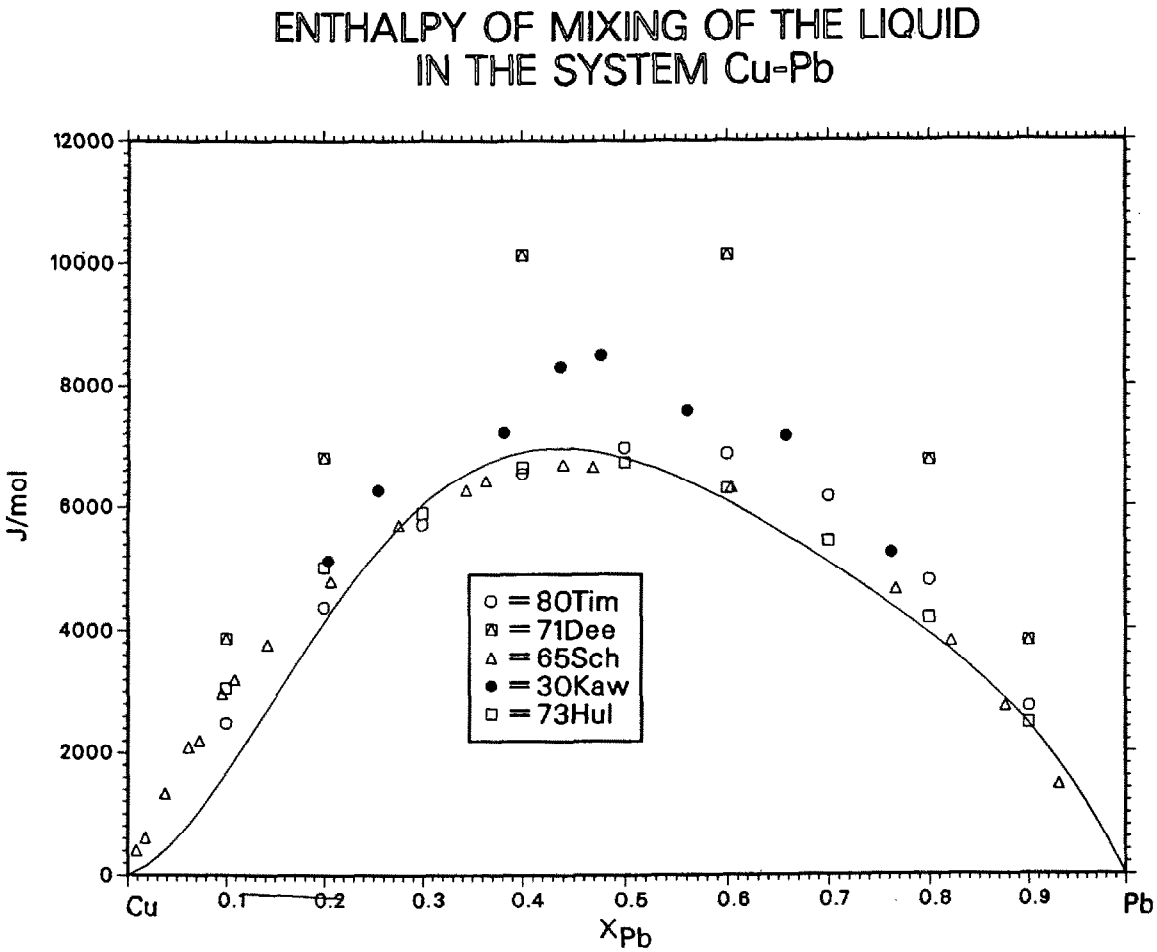

Fig. 4. The integral enthalpy of mixing of liquid copper–lead alloys: 73Hul [4] at 1473 K. 84Cha [6], 86Nie [7], 30Kaw [35] at 1473 K, 65Sch [29] at 1473 K, ——— this work (calculated, temperature independent); standard states Cu(l) and Pb(l).

the copper solid-solution field is not warranted. The maximum solid solubility of 0.4 at.% $[Pb]_{Cu}$ was found to be at the monotectic temperature 954.7 °C (1227.9 K). This valuation must be regarded as an upper limit for the solid solubility because of the assumption concerning the strict regular behaviour for the terminal solution. A similar rough estimate was obtained for the solid solubility of lead at the eutectic temperature, the calculations yielding a value of 0.0046 at.% $[Pb]_{Cu}$ at 326.5 °C (599.7 K).

Solution thermodynamics

The calculated integral enthalpy of mixing of liquid copper–lead alloys is shown in Fig. 4. The standard states were Cu(l) and Pb(l). The experimental points from the literature are also given in the graph. The assessed enthalpy

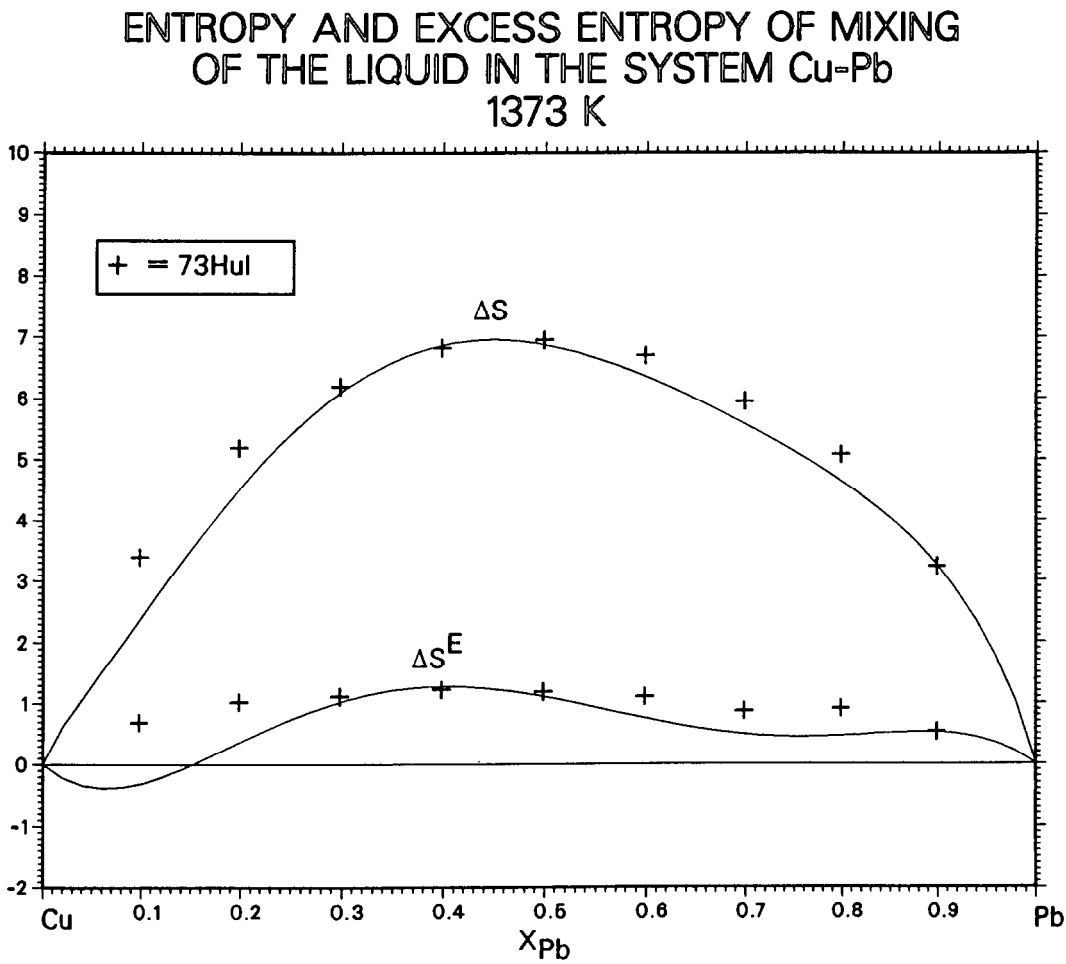

Fig. 5. Entropy and excess entropy of mixing of the liquid copper–lead alloys: 73Hul [4] at 1473 K, ——— this work (calculated, temperature independent); standard states Cu(l) and Pb(l).

of mixing of the molten alloy is endothermic with the maximum at 44 at.% Pb in the alloy. The experimental points of Deev et al. [30] are about 1–2 kJ mol^{-1} more endothermic than the assessed curve, which is in fair agreement with the points reported by Schürmann and Kaune [29] and Timucin [28]. Owing to their large scatter, the experimental points reported by Kawakami [35] were omitted in the final optimisation. The insufficient experimental information on the enthalpy of mixing of the molten alloy leads to the assumption of a temperature-independent enthalpy of mixing with $\Delta c_p = 0$. The optimised enthalpy of mixing is in good agreement with the assessment of Niemelä et al. [7].

The assessed entropy and excess entropy of mixing of the liquid alloy phase is shown in Fig. 5. The mixing entropy is also non-symmetric with the

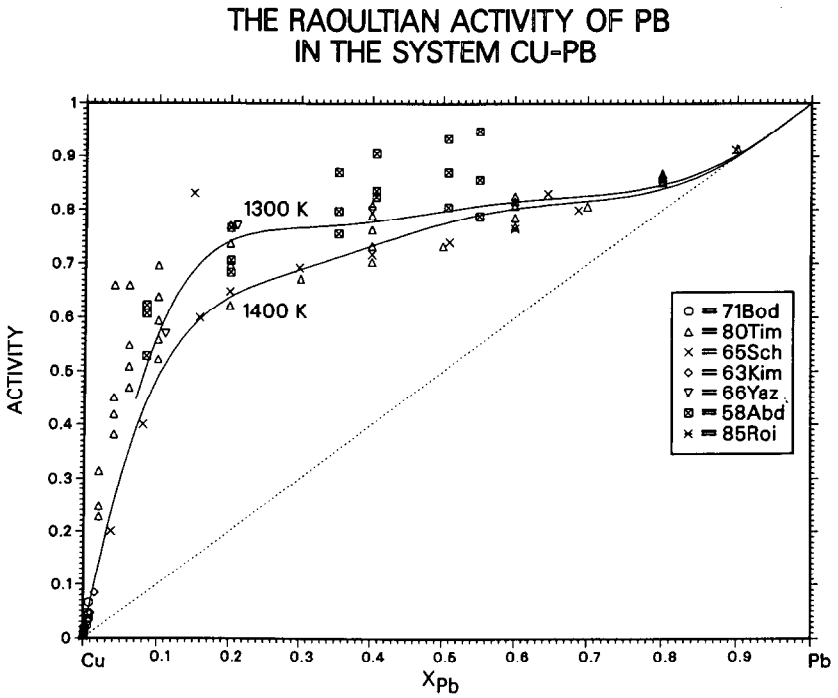

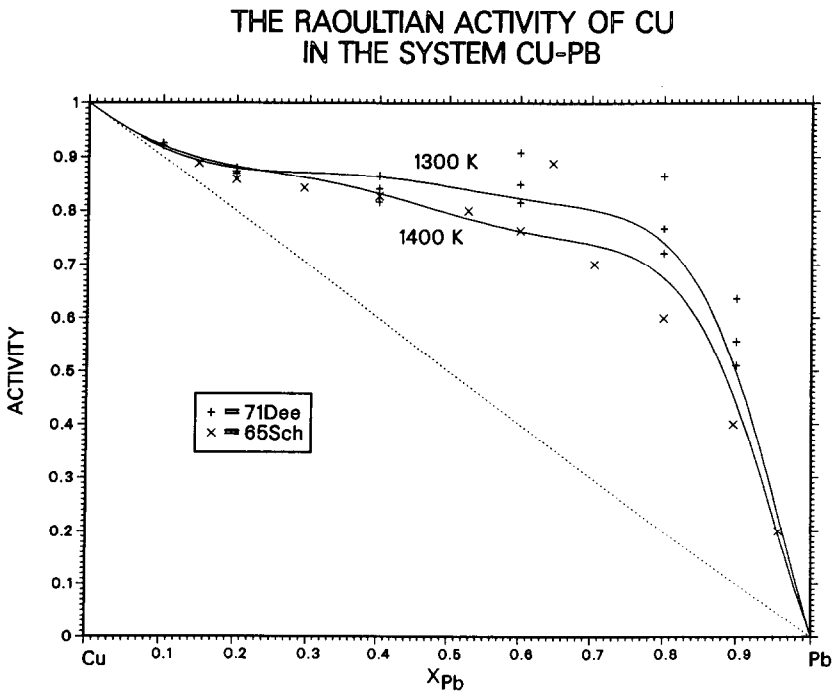

Fig. 6. Activities of copper and lead in the molten copper–lead alloy: 63Kim [19], 66Yaz [36], 71Bod [27], 71Dee [30], 80Tim [28], ——— this work at 1373, 1473 and 1573 K; standard states Cu(l), Pb(l).

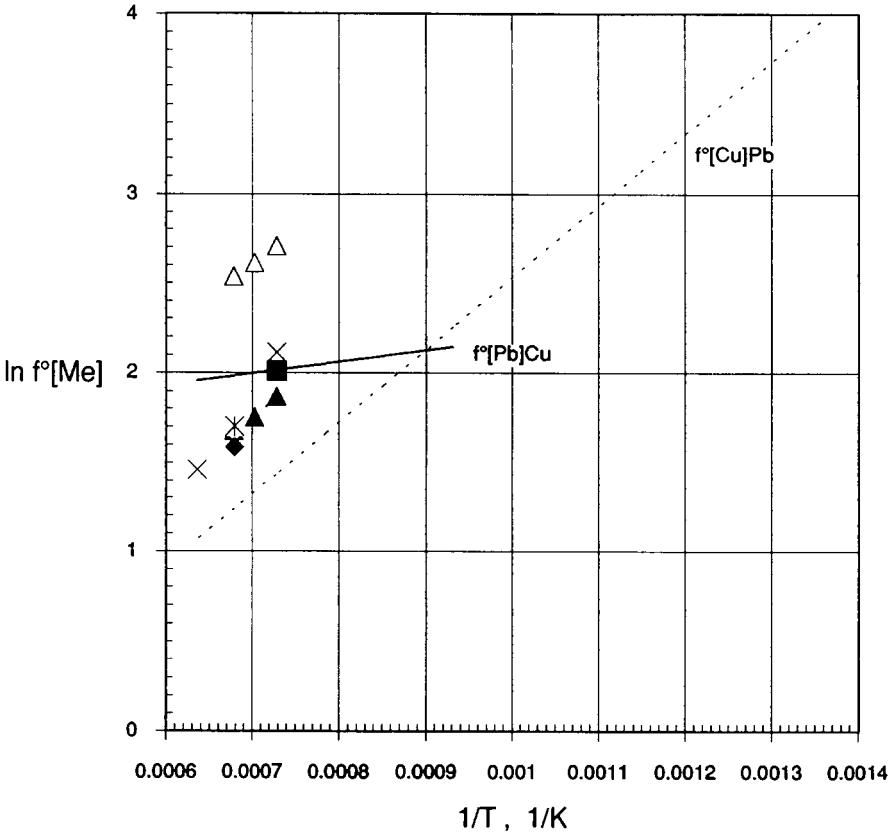

Fig. 7. The logarithmic activity coefficients of copper and lead in the molten alloy at infinite dilution as a function of the inverse absolute temperature: ▲ (Cu), △ (Pb) [28], ◆ [4], * [36], × [27], ■ [19], ——— $[Pb]_{Cu}$ and · · · $[Cu]_{Pb}$ this work; standard states Cu(l) and Pb(l).

maximum at 44 at.% [Pb]. The assessed values are in good agreement with the points reported by Hultgren et al. [4].

Figure 6 shows the assessed activity plotted against the composition of the molten alloy and their comparison with the observed values. The components show strong positive deviations from the Raoultian solution. The calculated activities are in good agreement with the vapour pressure data reported by Yazawa et al. [36] at 1100 °C and by Timucin [28] at 1000–1200 °C, who reported that at small concentrations of lead, however, there are larger deviations from the Raoultian behaviour than in the calculated curve. The activity values estimated by Schürmann and Kaune [29] on the basis of their enthalpy measurements are also close to the estimated plot. The experimental copper activities derived from the e.m.f. data of Deev et al. [30] also suggest larger deviations from ideality than those assessed in the present work. The activities given by Abdeev and Miller [23] show signifi-

cant systematic errors and scatter in the homogeneous alloys; their data were largely omitted in the final optimisation.

The limiting activity coefficients of the components at infinite dilution in liquid copper and lead can be calculated from the optimised set of data in Table 3. The following expressions were obtained for lead in copper and copper in lead, respectively

$$RT \ln f^{\circ}_{[Pb]Cu} \text{ (J mol}^{-1}) = 4794 + 13.124T \text{ (K)} \quad (5)$$

$$RT \ln f^{\circ}_{[Cu]Pb} \text{ (J mol}^{-1}) = 32532 - 11.850T \text{ (K)} \quad (6)$$

In eqns. (5) and (6), the standard states for the dissolved components were Cu(l) and Pb(l). The calculated limiting activity coefficients are shown in Fig. 7 together with the experimental information from the literature [4,19,21,27,28]. As one can see, the stronger temperature-dependence of the experimental activity coefficient of lead in copper, except in the case of the values of Timucin [28], suggests slightly smaller deviations from the Raoultian behaviour at high temperatures than the assessed value. The values of Timucin [28] for lead deviate systematically from the assessed values as well as from the other observations. The same is true of his copper activities determined by the Gibbs–Duhem integration from ${}^{Ex}\mu_{Pb}$. The reason for this systematic error is unknown.

SUMMARY

The least-squares optimisation of the experimental phase diagram and the thermodynamic information on the binary copper–lead system obtained using the Lukas program provided the following univariant points for the phase diagram: a eutectic point at ${}^{e}x_{Cu} = 0.0015$ and ${}^{e}t = 326.5\,^{\circ}C$; a monotectic equilibrium at ${}^{m}t = 954.6\,^{\circ}C$ with ${}^{m'}x_{Pb} = 0.18$ and ${}^{m''}x_{Pb} = 0.57$; a critical point of the liquid state miscibility gap at ${}^{cr}x_{Pb} = 0.31$ and ${}^{cr}t = 1007.0\,^{\circ}C$; a maximum solid solubility of lead in copper at the monotectic temperature with $x_{Pb} = 0.0040$.

The solid solubility of lead in copper is very low, less than 0.4 at.% at most at the monotectic temperature. The corresponding value in solid lead is much smaller, below 0.02 at.% $[Cu]_{Pb}$.

A thermodynamically consistent set of excess Gibbs energy functions for the solution phases was obtained in the least-squares analysis of the experimental data.

The limiting activity coefficients of lead in molten copper and copper in molten lead at infinite dilution were estimated from the optimised excess Gibbs energy of the alloy as follows

$$\ln f^{\circ}_{[Pb]Cu} = 1.58 + 576.6/T \text{ (K)} \quad (7)$$

$$\ln f^{\circ}_{[Cu]Pb} = -1.43 + 3913/T \text{ (K)} \quad (8)$$

with Cu(l) and Pb(l) as the standard states for the dissolved elements.

ACKNOWLEDGEMENTS

Financial support from the Academy of Finland and the Outokumpu Foundation for one of the authors (OT) is gratefully acknowledged. The authors are indebted to Dr H.-L. Lukas at the Max-Planck-Institut für Metallforschung, Stuttgart (F.R.G.), for providing the least-squares optimisation computer programs used in the calculations.

REFERENCES

1 M. Hansen and K. Anderko, Constitution of Binary Alloys, McGraw-Hill, New York, 1958.
2 R. Elliott, Constitution of Binary Alloys, First Supplement, McGraw-Hill, New York, 1965.
3 F. Shunk, Constitution of Binary Alloys, Second Supplement, McGraw-Hill, New York, 1969.
4 R. Hultgren, P. Desai, D. Hawkins, M. Gleiser and K. Kelley, Selected Values of the Thermodynamic Properties of Binary Alloys, American Society for Metals, Ohio, 1973.
5 R. Johnson, Bull. Alloy Phase Diagr., 1 (1979) 81–82.
6 D. Chakrabarti and D. Laughlin, Bull. Alloy Phase Diagr., 5 (1984) 503–511.
7 J. Niemelä, G. Effenberg, K. Hack and P. Spencer, Calphad, 10 (1986) 77–89.
8 Melting Points of the Elements, Bull. Alloy Phase Diagr., 2 (1981) 146.
9 Crystal Structures of the Elements at 25 °C, Bull. Alloy Phase Diagr. 2 (1981) 402.
10 K. Bornemann and K. Wagenmann, Ferrum, 11 (1913–1914) 291–293.
11 C. Chaib and J. Gasser, Z. Phys. Chem. NF, 156 (1988) 483–487.
12 A. Taskinen and H. Holopainen, H. Z. Metallkd., 71 (1980) 729–734.
13 V. Marcotte and K. Schroder, Cu–Pb–Sn Ternary System: Low Cu Additions to Pb–Sn–Binary System. in L. Bennett, T. Massalski and B. Giessen (Eds.), Mat. Res. Soc. Symp. Proc. Vol. 19: Alloy Phase Diagrams, pp. 403–410, North-Holland, Ser. A., New York, 1983.
14 C. Heycock and F. Neville, Phil Trans. R. Soc. London, Ser. A., 189 (1897) 25–69.
15 J. Taylor, Rev. Metall., 54 (1957) 950–970.
16 C. Pin and J. Wagner, Trans. AIME, 227 (1963) 1275–1281.
17 E. Pelzel, Metall., 10 (1956) 1023–1028.
18 E. Raub and A. Engel, Z. Metallkd., 37 (1946) 76–81.
19 G. Kim and M. Abdeev, Russ. J. Inorg. Chem., 8 (1963) 732–734.
20 E. Savitsky, Ju. Jefimov, T. Frolova, G. Omarova, Ch. Raub and H. Khan, J. Less-Common Metals, 83 (1982) 71–86.
21 A. Roine and H. Jalkanen, Metall. Trans., 16B (1985) 129–41.
22 J. Esdaile and J. McAdam, Proc. Aust. IMM, No. 239 (1971) 71–79.
23 M. Abdeev and O. Miller, Zh. Neorg. Khim., 3 (1958) 921–923.
24 A. Pelton and C. Bale, Metall. Trans., 17A (1986) 1057–1063.
25 H.-L. Lukas, E. Henig and B. Zimmermann, Calphad, 1 (1977) 225–236.
26 A. Dinsdale, SGTE Data for Pure Elements, National Physical Laboratory (UK), Report DMA(A) No. 195, 1989.
27 J. Bode, J. Gerlach and F. Pawlek, Erzmetall., 24 (1971) 480–485.
28 M. Timucin, Metall. Trans., 11B (1980) 503–510.
29 E. Schürmann and A. Kaune, Z. Metallkd., 56 (1965) 453–462; 56 (1965) 575–580.
30 V. Deev, V. Ribnikov, V. Goldobin and V. Smirnov, Zh. Fiz. Khim, 45 (1971) 3053–3056.
31 W. Seith, H. Johnen and J. Wagner, Z. Metallkd., 46 (1955) 773–779.

32 M. Vasil'ev, Inorg. Materials, 13 (1977) 156–157.
33 O. Kleppa and J. Weil, J. Am. Chem. Soc., 73 (1951) 4848–4850.
34 S. Briesemeister, Z. Metallkd., 23 (1931) 225–230.
35 M. Kawakami, Sci. Repts. Tohoku University, 19 (1930) 521–549.
36 A. Yazawa, T. Azakami and T. Kawashima, J. Min, Metall. Inst. Jpn., 82 (1966) 519–524.
37 J. Gorman and G. Preckshot, Trans. AIME, 212 (1958) 367–373.
38 A. Kirov, A. Boychev, E. Neykova, D. Denev and V. Bratanov, C. R. Acad. Bulg. Sci., 26 (1973) 1501–1504.
39 J. Esdaile, Metall. Trans. A, 13A (1982) 2097–2102.
40 E. Pelzel, Metall., 9 (1955) 692–694.